

# Performance of a diode-pumped 5 W Nd<sup>3+</sup>:GdVO<sub>4</sub> microchip laser at 1.06 μm

Chr.P. Wyss<sup>1</sup>, W. Lüthy<sup>1</sup>, H.P. Weber<sup>1</sup>, V.I. Vlasov<sup>2</sup>, Yu.D. Zavartsev<sup>2</sup>, P.A. Studenikin<sup>2</sup>, A.I. Zagumennyi<sup>2</sup>, I.A. Shcherbakov<sup>2</sup>

<sup>1</sup>Institute of Applied Physics, University of Bern, Sidlerstrasse 5, CH-3012 Bern, Switzerland  
(Fax: +41-31/631-37-65, E-mail: christian.wyss@iap.unibe.ch)

<sup>2</sup>General Physics Institute, Russian Academy of Sciences, 38 Vavilov street, Moscow 117942, Russia  
(Fax: +7-095/135-02-11, E-mail: zagumen@grow.mail.gpi.ru)

Received: 23 July 1998/Revised version: 9 November 1998/Published online: 24 February 1999

**Abstract.** GdVO<sub>4</sub> as a host for neodymium has several advantages for diode pumping in comparison with other crystals. The absorption cross section of neodymium in GdVO<sub>4</sub> is considerably stronger and broader than in YAG. This allows for the construction of very compact monolithic microchip lasers. In our paper, we report for the first time on a diode-pumped monolithic Nd<sup>3+</sup>(1.3 at. %):GdVO<sub>4</sub> microchip laser at 1.06 μm. A maximum output power of 5 W is achieved. The temporal and the spectral emission properties are described. The beam propagation properties are studied in detail.

**PACS:** 42.55.Rz; 42.60.-v; 42.60.Lh

Nd:YVO<sub>4</sub> and Nd:YAG are very efficient laser materials for diode pumping. There are a number of commercially available lasers with high efficiency and good beam quality. These materials are also used for the construction of compact microchip lasers [1–3]. Neodymium-doped GdVO<sub>4</sub> crystals are promising substitutes for Nd:YAG and Nd:YVO<sub>4</sub> in diode-pumped laser products [1]. It has been shown that Nd:GdVO<sub>4</sub> crystals have essential advantages for diode pumping in comparison with Nd:YAG. These advantages include the larger emission cross section ( $\sigma_e = 7.6 \times 10^{-19} \text{ cm}^2$  at 1.06 μm) and the more than 7 times larger absorption cross section ( $\sigma_a = 5.2 \times 10^{-19} \text{ cm}^2$  at 808 nm,  $E \parallel c$ ) of neodymium in GdVO<sub>4</sub> than in YAG [4, 5]. Due to the large absorption cross section of neodymium in GdVO<sub>4</sub>, it is possible to construct Nd lasers using very short laser crystals. Small monolithic Nd:GdVO<sub>4</sub> microchip lasers can be realised by coating the mirrors directly onto the surfaces of the crystal. Microchips allow for the construction of highly reliable, permanently aligned and very compact all-solid-state lasers.

A further advantage of Nd:GdVO<sub>4</sub> is the broad absorption with 3.2 nm FWHM of the pump transition at 808.4 nm. This results in a good spectral overlap between the diode-laser emission and the absorption of Nd:GdVO<sub>4</sub> without the need of diode-laser temperature control [5]. Also the large thermal conductivity of GdVO<sub>4</sub> with  $11.7 \text{ W m}^{-1} \text{ K}^{-1}$  along the (110) direction at 300 K is very favourable for efficient

crystal cooling [6]. The thermal conductivity is of GdVO<sub>4</sub> is more than a factor of two higher than that of YVO<sub>4</sub> and is even higher than that of YAG.

Recently more than 10 W power was reported with use of an end-pumped Nd:YVO<sub>4</sub> configuration [2]. In another Nd:YVO<sub>4</sub> laser using a face-cooling geometry, the beam quality was found to be nearly diffraction-limited ( $M^2 = 1.08$ ), but the output power did not exceed 2 W [3].

In Nd:GdVO<sub>4</sub>, however, there are only few papers reporting on laser action, despite of all the promising properties of GdVO<sub>4</sub> [5, 7–9]. Only output powers up to 800 mW are realised in CW and quasi-CW Nd:GdVO<sub>4</sub> lasers as yet [5]. Lasing in a monolithic Nd:GdVO<sub>4</sub> microchip has not yet been shown.

In our paper we report on a diode-pumped monolithic Nd<sup>3+</sup>:GdVO<sub>4</sub> microchip laser at 1.06 μm. The input–output curves are compared for two different excitation times. The spectral and the temporal behaviour are described. The divergence angle, the waist radius, and the beam propagation parameter  $M^2$  of the output beam are studied as a function of the pump power.

## 1 Experimental setup

The experimental arrangement is shown in Fig. 1. The diode-laser pump source (Fisba DL 50) emits a maximum power of 50 W at  $\lambda_p = 808 \text{ nm}$  in a bandwidth of 2 nm (FWHM). The

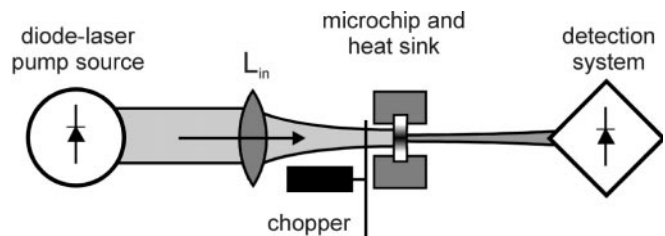


**Fig. 1.** Experimental arrangement. The resonator consists of a monolithic Nd<sup>3+</sup>(1.3 at. %):GdVO<sub>4</sub> microchip laser with mirror reflectances of  $R_{in} > 99.8\%$  and  $R_{out} = 99.5\%$

collimated beam is focused using an anti-reflection-coated lens  $L_{in}$  with a focal length of  $f = 50$  mm. The waist of the pump beam is located at the crystal front face. The variance in the spatial intensity distribution in the focus is  $\omega_p = 500 \mu\text{m} \pm 10\%$  and the divergence angle is  $12^\circ$  (FWHM). Due to the high absorption cross section in  $c$  axis polarisation ( $\alpha_{\text{peak}} = 78 \text{ cm}^{-1}$  ( $E \parallel c$ ),  $\alpha_{\text{peak}} = 10 \text{ cm}^{-1}$  ( $E \perp c$ ) in Nd (1.2 at. %):GdVO<sub>4</sub>) [5], the electric field vector of the linearly polarised pump beam is tuned to be parallel to the  $c$  axis of the crystal. The pump beam is chopped to reduce the thermal load in the crystal. The Nd<sup>3+</sup> (1.3 at. %):GdVO<sub>4</sub> microchip was grown at the General Physics Institute in Moscow by the Czochralski technique [5]. The optimal Nd<sup>3+</sup> concentration in GdVO<sub>4</sub> is not yet known. The dopant concentration is chosen on the basis of experiences in Nd:YVO<sub>4</sub> [1–3]. The 2.5-mm-long crystal with lateral dimensions of 5 mm × 5 mm is cut perpendicular to the  $a$  axis [10]. The incoupling mirror transmits more than 95% at the pump wavelength and reflects more than 99.8% at the laser wavelength. The mirror on the back surface of the crystal transmits 0.5% at 1.06  $\mu\text{m}$ . The transmission of the mirrors is not optimised. The length of the cavity is determined by the length of the crystal of  $L = 2.5$  mm. This yields an effective length of the resonator, considering the refractive index of GdVO<sub>4</sub> ( $n_e = 2.2$ ,  $n_o = 2.0$ ) [6] of  $L_{\text{reso}} \approx 5$  mm. The monolithical microchip is mounted on a water-cooled copper heat sink ( $T = 20^\circ\text{C}$ ) to allow for a proper cooling.

The dimensions of the whole setup are mainly dictated by the pump source. The overall length is 30 cm. To take advantage of the compact resonator, a high-power diode laser bar has to be butt-coupled to the crystal.

The beam is detected with either a power meter [Sensor Physics], a Germanium diode, a monochromator [Spectra Physics 500] in connection with a Ge-diode, or a CCD camera [Cohu 6700] in connection with a frame grabber. A selective filter is used to block the residual pump power.

## 2 Experimental results

The output power  $P_{\text{out}}$  as a function of the launched pump power  $P_{\text{in}}$  is shown in Fig. 2 for two different excitation times  $t = 1.6$  ms and  $t = 4.4$  ms. The duty cycle of the pump beam chopper is 8.1% and 5.5%, respectively. The laser

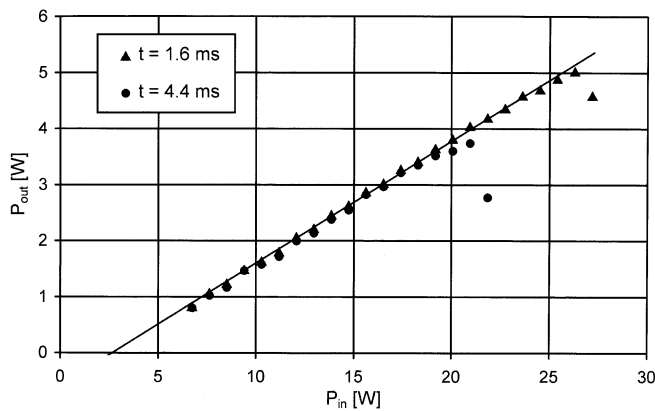


Fig. 2. Output power  $P_{\text{out}}$  as a function of the launched pump power  $P_{\text{in}}$  of a Nd<sup>3+</sup>:GdVO<sub>4</sub> laser at 1.06  $\mu\text{m}$  for two different excitation times  $t$

operates practically in CW regime due to the long excitation times compared with the lifetime of the upper laser level ( $\tau_e = 90 \mu\text{s}$ ) [5]. Therefore, threshold and slope efficiency are nearly the same for the two different excitation times. The threshold of the laser emission is  $P_{\text{th}} = 2.6$  W and the slope efficiency is 22%. The maximum output power achieved is 5.0 W. The threshold is quite high compared with Nd:YVO<sub>4</sub> [1–3]. This is mainly due to the large pump focus and the bad mode overlap. The low slope efficiency is believed to be a result of the non-optimised transmission of the output coupler.

During a pump pulse the laser emits CW. Due to the heating of the crystal by the pump beam, the output power is slightly decreasing ( $\approx 10\%$ ) during the first 10 ms after the leading edge of the pump pulse. The peak of the emission spectrum is located at 1063.2 nm and has a FWHM of 0.5 nm. Two small side bands ( $-12$  dB) are located on each side of the emission peak.

In Fig. 2 the output power drops off drastically for an input power of more than 21 W for  $t = 4.4$  ms and for more than 27 W for  $t = 1.6$  ms. The mirror on the front surface of the crystal was burnt by the pump laser leading to a decrease in output power. The longer excitation time leads to a higher temperature of the crystal.

Although the coating was burnt, the crystal itself was not damaged and was still lasing. Input power up to 20 W under true CW pumping did not destroy the crystal. With increasing pump power and under true CW operation, the cooling of a small crystal becomes a severe problem. The thermal flux can be enhanced by good thermal contact on a large surface. In order to enlarge the cooled surface, the crystal can be clamped between two diamond or sapphire plane plates [3]. An optimal thermal contact can be provided by mounting the whole stack in a flow tube.

Pictures of the output beam in two different distances from the microchip are taken. The intensity distributions are nearly Gaussian and circular within 20%. The variance of the spatial intensity distribution in the  $x$  direction is then calculated from each picture. According to the rules of a multi-mode Hermite-Gaussian beam a hyperbola is calculated from the two measured points yielding the waist radius  $\Delta r_x$  and the divergence angle  $\Delta \theta_x$  (half angle) of the output beam in the  $x$  direction. The relative error in  $\Delta r_x$  and  $\Delta \theta_x$  is  $\pm 10\%$  and the absolute error in the pump power is  $\pm 0.5$  W. Figure 3 shows  $\Delta r_x$  and  $\Delta \theta_x$  as a function of the launched pump power. With increasing pump power a growing number of resonator modes reaches the threshold for laser action. Therefore, the radius  $\Delta r_x$  of the beam waist becomes larger with increasing input power. Also the divergence angle  $\Delta \theta_x$  becomes larger with rising pump power  $P_{\text{in}}$ . The divergence angle is expected to increase with the numbers of resonator modes according to the same rule as the radius of the beam waist. But in Fig. 3 it can be seen, that the slope of the divergence angle  $\Delta \theta_x$  is smaller than the slope of the radius  $\Delta r_x$  as a function of the pump power. The observed effect is assigned to the thermal lensing of the heated crystal that leads to a reduction of the aperture angle of the output beam.

The beam propagation factor  $M^2$  is defined as

$$M^2 \equiv \frac{\pi \Delta \theta \Delta r}{\lambda}, \quad (1)$$

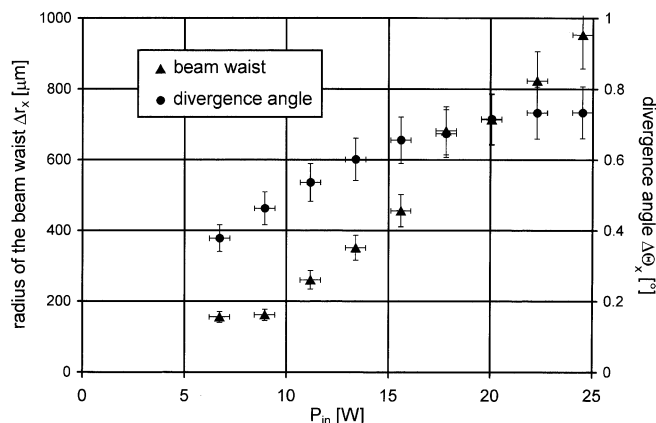


Fig. 3. Radius of the waist  $\Delta r_x$  (triangles) and divergence angle  $\Delta\theta_x$  (dots) of the output beam as a function of the launched pump power  $P_{in}$

with  $\Delta r$ : variance of the spatial intensity distribution,  $\Delta\theta$ : variance in the angular intensity distribution and  $\lambda$ : centre wavelength [11]. With the data from Fig. 3 we can calculate the  $M^2$  factor. The relative error in  $M^2$  is  $\pm 20\%$ . The beam propagation factor  $M_x^2$  in the  $x$  direction as a function of the pump power is shown in Fig. 4. The  $M^2$  values are ranging from 3 ( $P_{in} = 7$  W, duty cycle = 8.1%) to 36 ( $P_{in} = 25$  W, duty cycle = 8.1%). The small resonator length in our experiment results in a high  $M^2$ . The number of resonator modes is more than linearly increasing with increasing peak pump power  $P_{in}$ . The drastic increase in  $M^2$  is mainly due to the increase in the lasing volume. The relation between  $M^2$  and  $P_{in}$  contains therefore basically information about the inten-

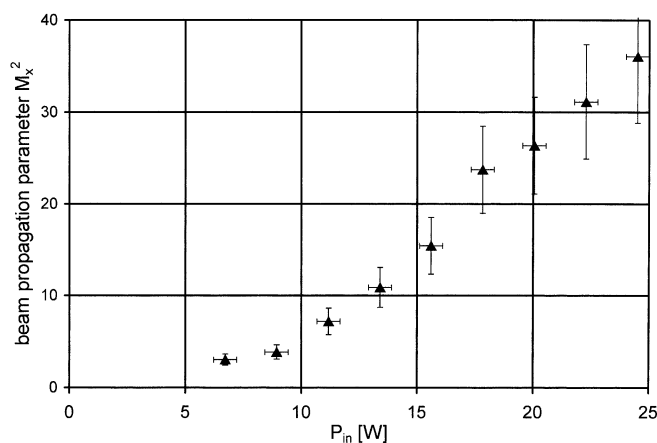


Fig. 4. Beam propagation parameter  $M_x^2$  of the output beam as a function of the launched pump power  $P_{in}$ . The solid line shows a fitted parabola

sity distribution in the focus of the pump beam. Information about the thermal lens can not be extracted.

### 3 Conclusions

A diode-pumped monolithic  $\text{Nd}^{3+}:\text{GdVO}_4$  microchip laser at 1.06  $\mu\text{m}$  has been built for the first time. The input-output curves have been measured for different excitation times. The slope efficiency is 22% and the threshold of the laser emission is 2.6 W. The mirror design has not been optimised. The highest output power achieved of 5.0 W is solely limited by the threshold of destruction of the mirrors on the crystal surfaces. The laser emits quasi-CW at 1063 nm into a bandwidth of 0.5 nm (FWHM). The divergence angle, the waist radius, and the beam propagation parameter  $M^2$  of the output beam have been studied as a function of the pump power.  $M^2$  is increasing with increasing pump power from 3 ( $P_{in} = 7$  W, duty cycle = 8.1%) to 36 ( $P_{in} = 25$  W, duty cycle = 8.1%).

The efficiency of the  $\text{Nd}:\text{GdVO}_4$  laser can be further enhanced by optimising the mirror transmission and the pump geometry. Further, a better cooling system can improve the beam quality. Although the performance of the  $\text{Nd}:\text{GdVO}_4$  laser is not yet as good as that of  $\text{Nd}:\text{YVO}_4$  and  $\text{Nd}:\text{YAG}$  lasers,  $\text{GdVO}_4$  is a possible substitute for these materials.

*Acknowledgements.* This work was supported in part by the Swiss Priority Program "OPTIQUE II", by the Swiss National Science Foundation under contract no. 7 IP 051215 and by the Russian Foundation for Basic Research under project no. 98-02-17581. Chr. Wyss acknowledges help in the laboratory by Anna Lüdi.

### References

1. L. DeShazer: *Laser Focus World* **30**, 88 (1994)
2. J. Zhang, M. Quade, K.M. Du, Y. Liao, S. Falter, M. Baumann, P. Loosen, P. Poprawe: *Electron. Lett.* **33**, 775 (1997)
3. D.C. Brown, R. Nelson, L. Billings: *Appl. Opt.* **36**, 8611 (1997)
4. A.I. Zagumennyi, T.D. Zavartsev, P.A. Studenikin, I.A. Shcherbakov, F. Umyskov, P.A. Popov, V.B. Ufimtsev: *Proc. SPIE* **2698**, 182 (1996)
5. T. Jensen, V.G. Ostroumov, J.P. Meyn, G. Huber, A.I. Zagumennyi, I.A. Shcherbakov: *Appl. Phys. B* **58**, 373 (1994)
6. P.A. Studenikin, A.I. Zagumennyi, Yu.D. Zavartsev, P.A. Popov, I.A. Shcherbakov: *Quantum Electron.* **25**, 1162 (1995)
7. J.V. Klimov, V.B. Tsvetkov, I.A. Shcherbakov, J. Bartschke, K.J. Boller, R. Wallenstein: *OSA Trends Opt. Photon. Adv. Solid State Laser* **1**, 438 (1996)
8. A.J. Alcock, J.E. Bernard: *Proc. of the LEOS '95* (cat. No. 95CH35739) **2**, 186 (1995)
9. J. Bartschke, I.V. Klimov, K.J. Boller, R. Wallenstein: *Proc. of the CLEO '95* (Cat. No. 95CH35800), 126 (1995)
10. I.A. Shcherbakov, A.I. Zagumennyi: *Proc. of ALT '94, Laser Methods of Surface Treatment and Modification*, Konstanz, Germany, SPIE **2498**, 241 (1994)
11. A.E. Siegman: *Lasers* (University Science Books, Mill Valley CA 1986)